Proceedings World Geothermal Congress 2020+1
Reykjavik, Iceland, April - October 2021

# Hydrogeological and Geothermal Features of Thermal and Mineral Water of Çamlıdere (Ankara-Turkey)

Pasvanoğlu S[1] and Çelik M[2].

[1]Yahya Kaptan Mah. Kocaeli-Izmit, Turkey

[2]Ankara University, Geological Eng. Dept. 06830 Gölbaşı, Ankara, Turkey

E-mail address, spasvanoglu@hotmail.com

**Keywords:** Thermal waters, hydrogeological, Çamlıdere, Central Anatolia, Turkey

## ABSTRACT

Chemical and isotope compositions of water samples collected between 2013 and 2014 from 26 springs and wells located in the Çamlıdere region (Ankara, Turkey), were examined. The main objective of the work was to characterise geothermal resources to be exploited in the future. Geothermal springs at Çamlıdere occur in an area of Miocene volcanics consisting of altered andesites, basalts and pyroclastic products. Thermal waters from Çamlıdere area are of Na-$HCO_3$ and Ca-Na-$HCO_3$ type waters with temperatures>42 °C, while cold waters are mostly of Ca-$HCO_3$ type with low ion content. Geochemical processes responsible for the genesis of the hydrochemical features of the waters include dissolution, mixing, and ion exchange. Reservoir temperatures were estimated, and the results indicated that water-rock equilibrium was not attained. The total natural heat discharge is low (< 1 MW th for all thermal springs and up to approximately 6 MW for all artesian wells. The estimates indicate a system with a limited convective flow. The isotopic data of Çamlıdere water indicates their deep-circulating meteoric origin and allow estimation of infiltration altitude ranging between 1494 and 1833 m a.s.l. The Çamlıdere system is a low-temperature, fracture-zone system that has developed as an advective geothermal system.

## 1. INTRODUCTION

Located, in Central Anatolia GVP, one of the four main Neogene and Quaternary volcanic fields of Turkey, comprises a number of composite volcanic province intimately associated with the development of a series of sedimentary basins Toprak et al., (1996). The northern margin of the GVP is bordered by the Northern Anatolian Fault Zone (NAFZ).

The Çamlıdere prospect is located 100 km NW of Ankara (Central Anatolia Fig 1) and hosted in the Tertiary GVP (sometimes called Köroğlu). The area of study has an average elevation of 1065 m a.s.l and a maximum elevation of 2040 m a.s.l at Mahya Mountain (Fig 1). Mahya Mountain is interpreted as a stratovolcano based on morphology Türkecan et al. (1991).

Active tectonics and young volcanoes in the Çamlıdere region have led to the formation of numerous hot and mineral sources. Thermal waters are discharged by springs in and around the town of Çamlıdere and emerge through the faults and fracture zones of the Köroğlu Volcanic Complex.


**Figure 1. Location map of the study area. Water numbers refer to the sample site number in Table 1.**

The thermal and mineral springs have temperatures ranging between 11–28 °C and occur at Muzrupağacın, Ahatlar, Atça, Tatlak and Sarıkavak. Drilling of four artesian wells encountered thermal water with flow rates of 8 and 46 L/s and temperatures of 27 and 42 °C at Ahatlar and Muzurupağacın, respectively.

Chemical and isotope compositions of water samples collected between 2013 and 2014 from 26 springs and wells located in the Çamlıdere region were examined. The field survey allowed the identification of several spring discharges, namely the ones referred to as ÇT-6, ÇT-7, and ÇT-8 (Table 1).

Other discharges already identified in the literature were also analysed (ÇT-5, ÇT-9, ÇT-10, ÇT-11 and ÇT-12). Four water samples were collected from geothermal wells (ÇT-1, ÇT-2, ÇT-3 and ÇT-4) at Ahatlar and Muzrupağacın. Samples were collected from 13 cold water sampling points (ÇS-1-9, ÇS-11 to 14), a representative sampling of the local groundwater system (Table 2).

In addition, one water sample was collected from Kuşçular lake (ÇS- 10), representative of the surface water in the area.

## 2. GEOLOGY

The Çamlıdere basin is enclosed by several large active faults and is characterised by caldera and volcanic vents. The volcanic rocks that consist of a series of andesites, basalts, and their pyroclastics form the largest geological unit in the area (Fig. 2).

The internal structure of volcanics is characterised by at least nine major volcanic eruption centres including the Ovacık volcanic complex (NW Çamlıdere) which is centred on a caldera, of about 5 km in diameter Toprak et al. (1996) and the Mahya volcanic complex west of Çamlıdere region.

The volcanic activity seems to have started with lava flows; the earliest lava flow took place in Palaeocene-Eocene age as lower lava of aa-type plateau basalt with a thickness of 250–400 m Erişen and Ünlü (1980) (Fig 2).

Aa lavas are overlain by intercalated andesitic-basaltic lava flows (Upper Miocene age) and pyroclastic products (lahar volcanic breccia, lava, tuffs and agglomerates) of eruptions from single centred volcanoes (Fig 2). The andesitic basaltic lava flows are interlayered with lacustrine sediments of the Pazar Formation.

Following the phase of volcanism, extensive lakes and related basins became dominant across the whole of Central Anatolia as separate basins. The andesitic-basaltic lava flows are unconformably overlain by the Pliocene acidic lava flows and domes of the Upper lavas (altered rhyolites, trachytes and glassy tuff).

Localised lacustrine units of Sinap Formation have formed as a result of the regional uplift starting in the Pliocene together with Quaternary deposit at the top which unconformably covers the Köroğlu volcanics. The basement beneath the province consists of Paleozoic schists and Permo-Triassic limestones Erol (1954).

The Mesozoic units consist mainly of Lower Cretaceous limestone (250-500 m thick, lying 22 km NE and 30 km NW of the Çamlıdere) and Upper Cretaceous flysch facies, that cover the Paleozoic basement and is overlain by Köroğlu Volcanics Erişen and Ünlü (1980).

The volcanic activity which built up this province is reported to have started at the end of the Upper Cretaceous but reached its climax during the Miocene Güleç (1994).

## 3. HYDROGEOLOGY

Thermal springs discharge in volcanic terrain, often in clusters, along faults in 5 separate areas. Ahatlar, Atça, Muzrupağacın, Tatlak and Sarıkavak are important mineral waters in the area (Fig 3). The spring discharge temperatures are between 11 and 28 °C. The artesian flow of four wells (depths 100 to 1367 m) discharges thermal waters with temperatures changing between 27 and 42 °C.

At Ahatlar, which is located about 10 km west of Çamlıdere (Fig 1 and 3), there are numerous thermal-mineral springs mostly emanate from the fractures and fault zone with different discharge rate and temperatures. In their natural state, spring discharges in the region are identified by brown-stained seeps, and gas (presumably $CO_2$) and mineral water discharge in stream beds.

The thermal springs emerge along a 300 m-long section of the Ahatlar Stream. The discharge rate varies between 0.01 and 0.1 L/s, with temperatures ranging between 23°C and 27°C. The Ahatlar Stream (no ÇT-12) mineral water is one of spring water that is issued from an intersection point of an N45°W trending fault and a fault which has approximately an E-W direction within the Ahatlar Stream Pasvanoğlu and Çelik (2019).

Based on geological and geophysical data, for the Ahatlar region, two artesian waters (ÇMJ-1 and ÇMJ-2) have been obtained from the IL Bank wells drilled in 2009. At the ÇMJ-1 well, the flow rate is 46 L/s, the temperature is 27°C and the depth is 103 m. The ÇMJ-2 has a flow rate of 9 L/s with a temperature of 42°C discharging from a depth of 274 m (Figs. 1B and 3).

The distance between the two wells is 5 m. The Ahatlar -Çamlıdere reservoir developed along a long fault and fracture zone in the volcanic units; the two production wells affect each other due to their limited separation. These wells have been constantly discharging without control to the Ahatlar Stream and into agriculture areas due to their damaged and punctured casing.

The Muzrupağacın spring (ÇT-5) is located 8 km away from Çamlıdere to the southwest and is also an important water source for the area (Fig. 1 and 3). The thermal waters have a temperature of 25°C and have a total flowrate that varies seasonally from 0.5 to 1 L/s. $CO_2$ also emanates with the water in an area of 5m$^2$ on the Muzrupağacın spring.

The springs at Muzrupağacın discharge along a fracture zone that is inferred to be an extension of the fault network to the NE from which the Ahatlar Stream mineral springs discharge. The fault system acts as a conduit through which Muzrupağacın waters discharge at the surface.

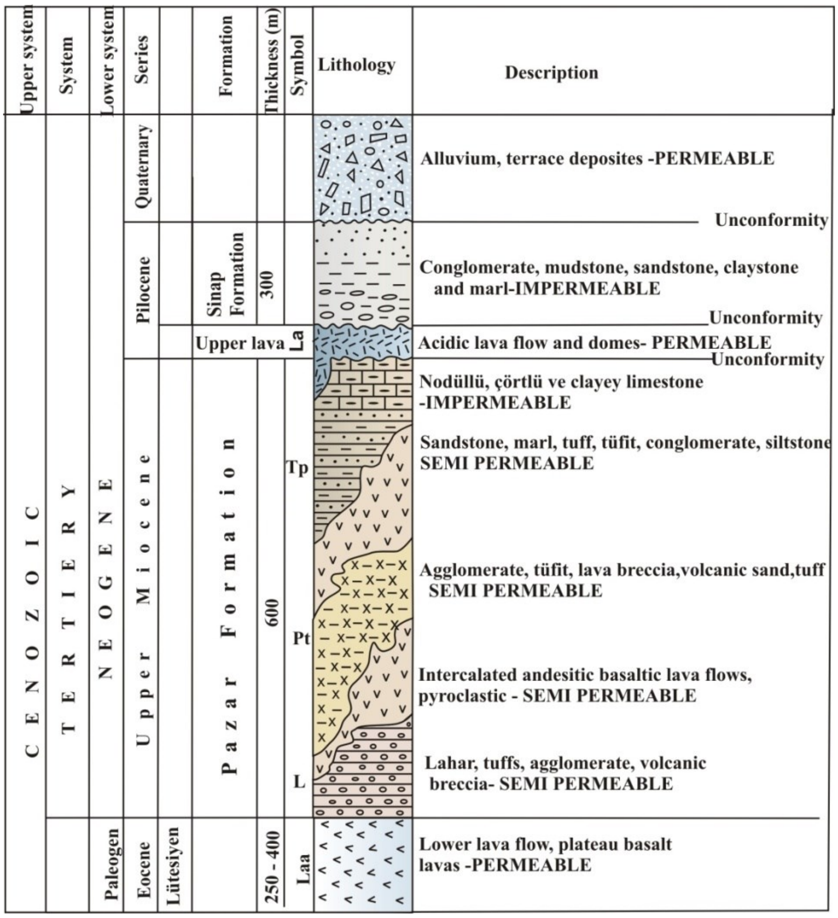


**Figure 2. Stratigraphic columnar section of the research area**

Thermal spring waters at Muzrupağacın dried up after two MTA wells were drilled relatively close to the spring. The ÇT-5 spring and MTA wells are located within an altitude range of 1150 and 1039–1078 m a.s.l., respectively. Artesian waters have been obtained from two MTA wells (AÇT-1 and AÇT-2, Fig 1).

At the AÇT-1 geothermal well (no ÇT-3), the discharge is 8 L/s, the temperature is 40°C, and the depth is 1020 m. The well encountered a temperature of about 80.5°C at the well bottom Bülbül et al. (2012). The AÇT-2 well (sample no. ÇT-4) produced hot water with a flow rate of 11 L/s at a temperature of 37°C at a depth of 1367.5 m.

The bottom hole temperature of AÇT-2 well is 97.5°C Bülbül et al. (2013). The flow rate of the thermal water stimulated with a compressor at 200, and 300 m depth was 17 and 26 L/s, respectively. In addition, 10 km away from Çamlıdere towards the SW, there are three thermal water springs in Sarıkavak village with flowrates ranging between 0.05 and 1 L/s and discharge elevation between 1016 and 1100 m.

These thermal springs are called Sarıkavak Uyuz (ÇT-6), Ilıca (ÇT-7) and Sarıkavak Kökderesi (ÇT-8)(Fig. 1 and 3). The temperature of these waters is between 22°C and 28°C. Also 17 km away from Çamlıdere towards the southwest, there is Tatlak mineral water (ÇT-9) in Tatlak village with a temperature of 23°C and discharge of 1 L/s (Fig 1 and 3).

This water is issued through a stream bed, and discharge elevation of the spring is 1035 m. Carbonate precipitates can be observed in surface exposure. Two mineral springs (ÇT-10 and ÇT-11) are located near the village of Atça, 6.5 km west-northwest of Çamlıdere (Fig. 1 and 3). Mineral spring waters issue from an N-S trending fault.


**Figure 3. Thermal and mineral waters in the Çamlıdere area. a) Ahatlar ÇT-1 & ÇT-2 geothermal well, ÇT-12 Ahatlar mineral spring, b) Ahatlar ÇT-1 geothermal well; c) ÇT-5 Muzrupağacın thermal spring water; d) ÇT-9 Tatlak mineral spring; e) and f) ÇT-10 and ÇT-11 Atça mineral spring waters; g) ÇT-8 Sarıkavak Kökderesi spring; ÇT-9 Sarıkavak Uyuz spring water and i) Silica precipitation around Sarıkavak Kökderesi spring water**

The water discharge from two shallow (6–7 m depth) wells with a temperature range of 11–13°C and discharge at elevations ranging from 1096 to 1102 m a.s.l.; the distance between the two wells is 20 m. It was observed that there was interference between the wells during a pumping test.

The temperature and flow rate of the Atca (ÇT-11) mineral spring is 13°C and 3.5 L/s, respectively; $CO_2$ gas is also emanating with the water. The hydrogeological structure of the Çamlıdere thermal prospect is largely controlled by the extension of the NAFZ. The Çamlıdere region appears to be located in the shear zones of the fault systems developed in two tectonic directions.

The region has been exposed to numerous tectonic and volcanic processes that play an important role in the hydrodynamics of the reservoirs. To the east, NE and to the NW of the study area, the Lower Cretaceous limestone is exposed over wide areas lying 22 km NE and 30 km NW of the Çamlıdere. The Lower Cretaceous limestones lie unconformably over metamorphic rocks Erişen and Ünlü (1980).

The aa-type plateau basalts formed by fissure eruption are permeable. Open fractures are the conduit for the upward migration and discharge of the thermal waters originating from the deep circulation of meteoric water. Agglomerates also possess good permeability features. The andesitic-basaltic units inferred as intercalated lava are evaluated as semi-permeable.

Two cap rocks have been identified in the Çamlıdere, Pazar and Sinap Formations. The Pazar Formation has a thickness of 600 m and is composed of carbonate-cemented conglomerate, sandstone, marl, tuffs, siltstone; coal beds add silt and agglomerates. This well-bedded formation has low porosity and likely represents an impermeable cap to the underlying geothermal reservoir.

The Pliocene Sinap Formation is up to 300 m thick and overlies unconformably on the Upper lava in the Çamlıdere basin. Alternation of Pliocene mudstone, sandstone, claystone and marl also caps the geothermal system containing heat and maintaining water pressure. Impermeable units within the spring areas tend to restrict groundwater flow to overlying units.

The alluvial material of Quaternary units, pyroclastic and lacustrine sediments (sandstone and conglomerate) of the Sinap Formation is considered to possess favourable infiltration characteristics as part of the recharge area.

Based on resistivity measurement and drilling log conducted in the Ahatlar and Muzrupağacın region ILBank (2009); Bülbül et al. (2012, 2013), it has been determined that no impermeable rocks of sufficient thickness exist in this area.

The caprock has low inherent permeability. Still, it is transected by a number of faults, damage zones, and fractures, which provide leakage to the surface – so the 'system' does not have an impermeable cap, although unfractured strata have low permeability. The Köroğlu volcanism forms the heat source in the geothermal area.

## 4. GEOCHEMICAL STUDIES

### 4. 1 Water chemistry

Thermal and mineral waters in Çamlıdere are near neutral, with pH ranging from 6.20 to 7.80 (Table 1). Electrical conductivity varies from 335 to 3550 µS/cm. Most samples of springs and thermal wells in Table 1 are 'mineral bicarbonate waters' since their $HCO_3$ content is>600 mg/L. The definition would also bring cold spring ÇS-5 into the 'mineral water' group (Table 2).

From an interpretation of the Piper diagram (Fig. 4), it can be noted that the thermal and cold waters clearly plot in distinct fields. The chemical composition of the groundwater investigated is from freshwater to alkaline along the long flow path. The cold waters are characterised dominantly as Ca-Mg-$HCO_3$ type, largely as a function of their host rocks.

According to the concentrations of major cations and anions, the thermal and mineral water composition varies from Ca-Na-$HCO_3$ to Na-$HCO_3$ type (Fig. 4). Their water types are a result of rock dissolution and ion exchange reactions in the aquifer at lower temperature Pasvanoğlu and Çelik (2019).

The composition of ÇT-1, ÇT-9 and ÇT-11 mineral bicarbonate and thermal waters seems to point to mixing of these waters with high salinity fluids that circulate at depth, probably in Mesozoic carbonates, and then upwell along with the major fractures (Fig 4). The high concentrations of $HCO_3^-$, $K^+$, and $Na^+$ are produced by the hydrolysis reaction of dissolved $CO_2$ with the rocks (e.g., with K-feldspar in Eq. (1).

This also explains the alkaline nature of the waters: $2KAlSi_3O_8 + 2CO_2 + 3H_2O \leftrightarrow A_{l2}Si_2O_5(OH)_4 + 2K^+ + 2HCO_3^- + 4SiO_2$ (1)

Further, the ratio of Na/K in solution is controlled by temperature-dependent reactions such as in Eq. (2):

$NaAlSi_3O_8 + K^+ \leftrightarrow KAlSi_3O_8 + Na^+$ (2)

High bicarbonate concentrations are due to the reaction of circulating $CO_2$-rich meteoric waters reacting with limestone forming $CO_2$-rich waters, and possibly from the magmatic fluid. The EC content of ÇT-11 mineral water is greater than all waters in Çamlıdere area (Table 1).

The $Ca^{2+}$, $Mg^{2+}$ concentrations in the ÇT-11 spring are the greatest in waters with elevated $HCO_3$ concentration. This shows that the Atca (ÇT-11) mineral spring is enriched in $Ca^{2+}$, $Mg^{2+}$ and $HCO_3^-$ inferred to be due to dissolution of carbonate rocks such as calcite, and input of endogenous $CO_2$ in the study area.

The discharge waters in the ÇT-11 mineral spring are alkaline and much more mineralised than all other waters in the Çamlıdere prospect. In the Ahatlar ÇT-1 (ÇMj-1) geothermal well and Atca (ÇT-11) mineral waters due to connectivity to the deep source, the additional impact of the greater $Cl^-$ can be observed (Table 1).

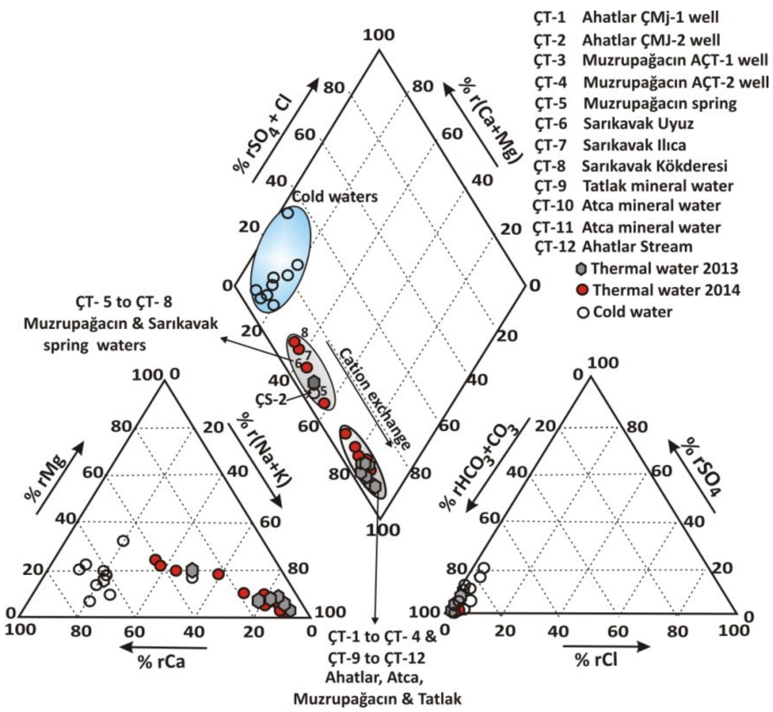


**Figure 4. Piper diagram showing major ion composition in the Çamlıdere area.**

These two waters have the highest chloride content supporting them being most representative of the deep fluid Pasvanoğlu and Çelik (2019). Increase in $Cl^-$ level may be associated with the leaching of rocks in the course of long subsurface circulation of the water. Conductive cooling following mixing is thought to be responsible for the low temperature of Ahatlar waters.

The waters from Muzrupağacın and Sarıkavak (ÇT-5 to ÇT-8) springs that emerge from the volcanics have salinities low enough to indicate that they circulate in the shallow aquifers that emerge at low pressures, possibly from secondary fractures. Muzrupağacın spring (ÇT-5) and Sarıkavak (ÇT-6 to ÇT-8) spring waters are Ca-Na-$HCO_3$ type waters.

The concentration of $Na^+$, $Cl^-$ and $HCO_3^-$ ions in springs ÇT-5, 6, 7 and 8 are almost the same (Table 1). Low chloride values in this type of waters are consistent with surface meteoric waters.

The Tatlak (ÇT-9) thermal water was also characterised by high $Na^+$, $Ca^{2+}$, $HCO_3^-$, $Cl^-$ and $SiO_2$, and EC (1816 to 2250 µS/cm) content which indicates relatively longer circulation and residence times, similar to Ahatlar and Atca thermal and mineral waters (Table 1).

The $SiO_2$ concentration in thermal waters (38.48 - 141 mg/L) is greater than that of the cold waters, which reflects the reaction of the aquifer with silicate minerals in the reservoir rocks (Table 1). The increases of alkalinity and pH, as well as the high concentrations of monovalent cations, point to intense alteration processes.

The studied waters are also enriched in $F^-$ (6.10 -7.31 mg/L) and B (5.80-6.92 mg/L). The high $Na^+$, $HCO_3^-$, $K^+$, $Cl^-$, $SiO_2$ and $F^-$ contents have been derived, through water-rock interaction, almost totally from the nearby volcanics. Lithium contents in Muzrupağacın and Sarıkavak thermal waters (ÇT-5 to ÇT-8) are lower than in both Ahatlar geothermal wells and Atca waters.

This indicates that the pathway of thermal spring and geothermal well waters at Ahatlar and Atca is longer than all other waters. However, the concentration of lithium is low in both areas which suggest that there is probably the interaction with reservoir rocks during fluid ascent, where lithium is incorporated into hydrothermal alteration products.

### 4. 2 Geothermometer

The estimates obtained from two different quartz geothermometers (119–149°C and 121–157°C) are almost the same, differing from each other by a maximum of ± 7°C (Table 3). The quartz temperature is 122°C and 125°C for Ahatlar geothermal well (no ÇT-1); the most representative of the deep fluid in this area.

The K-Mg temperatures range from 69°C to 129°C and agree well with those obtained from the silica geothermometers The K-Mg equilibrium temperature for two geothermal end-member samples (ÇT-1 and ÇT-11) are rather close, namely 129 and 113°C, respectively (Table 3).

The observed $SiO_2$ values and inferred T(K-Mg) data indicate some advective (terrain controlled) shallow flow involving $SiO_2$ re-equilibration of mixed thermal fluids.

**Table 3. Results of geothermometers of the study area**

| Geothermometer (°C) | ÇT-1 | ÇT-2 | ÇT-3 | ÇT-4 | ÇT-5 | ÇT-6 | ÇT-7 | ÇT-8 | ÇT-9 | ÇT-11 | ÇT-12 |
|---|---|---|---|---|---|---|---|---|---|---|---|
| T °C$_{measured}$ | 42 | 27 | 40 | 38 | 25 | 28 | 25 | 22 | 23 | 11 | 23 |
| A-Christobalite | 74 | 106 | 96 | 72 | 87 | 71 | 70 | 82 | 86 | 80 | 97 |
| Quartz[1]$_{no\ steam\ loss}$ | 125 | 157 | 146 | 123 | 137 | 122 | 121 | 133 | 137 | 130 | 148 |
| Quartz[1]$_{max.steam\ loss}$ | 122 | 149 | 140 | 120 | 133 | 120 | 119 | 129 | 133 | 127 | 142 |
| Chalcedony[1]$_{no\ steam\ loss}$ | 97 | 133 | 121 | 94 | 111 | 93 | 93 | 106 | 110 | 103 | 122 |
| K-Mg [2] | 129 | 107 | 105 | 102 | 81 | 88 | 69 | 73 | 110 | 113 | 110 |

Like Fig. 5 Na-K-Mg Giggenbach diagram, in Fig. 6, the positions of the samples do not indicate any equilibration between the rock and waters. Two trends are emanating from the position of the high $Cl^-$ waters (ÇT-1 and ÇT-11) indicated in Fig. 6 to reach the full equilibrium line of deep fluids.

Namely a: the vertical trend from ÇT-3 to ÇT-1 continues (indicating deep high reservoir temperature of about 220°C) or b: a 'tilted' trend from ÇT-9 to ÇT-11 becoming dominant indicating a deep reservoir temperature of about 140°C that could dominate the lower reservoir.

The relative Mg-Ca contents correspond to temperatures close to those measured or indicated by quartz and K-Mg contents; relative Na-K contents suggest deep water-rock equilibration temperatures of about 220 °C. Hence, this geothermometer proposes an estimated Na/K equilibrium temperature of 220 °C supporting the temperatures suggested by the Na-K-Mg geothermometer (Fig. 5).

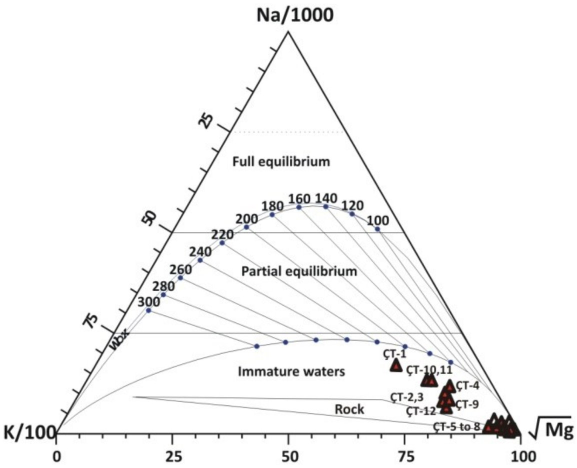


**Figure 5. Na-K-Mg Giggenbach diagram**

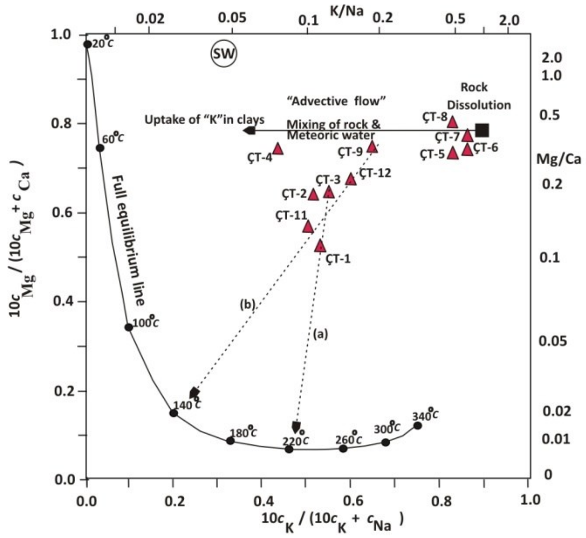


**Figure 6.Cross plot of 10Mg/(10Mg+Ca) vs 10K/( 10K+Na) for thermal and mineral waters discharging from Çamlıdere area.**

In the model given above, sample ÇT-1 is believed to be the most likely water representing the deep reservoir fluid. First, ÇT-1 (Ahatlar ÇMJ-1 well) is one of the waters having high $Cl^-$ content. In addition, the same water has the closest position to the full equilibrium line in the Na-K-Mg-Ca diagram (Fig 6).

ÇT-1 yield 97 °C and quartz geothermometer (with and without steam loss) yield 122 °C and 125 °C, respectively. The K-Mg geothermometer of Giggenbach (1988) also yields a similar temperature for the same water: 129 °C. These results were consistent with the temperature measured in the bottom hole temperature (AÇT-2: 97.5 °C) of ÇT-4 geothermal well at a depth of 1367.50 m.

The values obtained for the thermal mineral bicarbonate waters suggest that the reservoir is filled with low to middle enthalpy waters, probably because the convection occurring in the unconfined area of the reservoir reduces the thermal gradient. As shown by chemical geothermometry and temperatures recorded in geothermal wells, the Çamlıdere prospect is a low-enthalpy geothermal system.

### 4.3 Reservoir assessment

The Çamlıdere thermal prospect is a low-temperature system with reservoir temperatures about 100 °C at a depth of 1367.5 m. The down-hole temperature-profiles of the two deep wells are not known, but one could use geothermometer data to assess models of heat transfer.

Using the simple reservoir assessment described by Hochstein (1975) with reference to a mean annual temperature of 11.5 °C, the anomalous heat discharge of the four artesian wells and thermal springs listed in Table 1 can be estimated and were found to be about 6 MW and about 0.3 MW, respectively. The estimates indicate a system with limited convective up-flow.

The high bottom-hole temperature at ÇT-3 and ÇT-4 can be 'normalised' with respect to the inferred annual To at each site. This yields an apparent gradient of about 86 °C/km at ÇT-3 and about 63 °C/ km at ÇT-4.

### 4.4 Isotopic Signatures

4.4.1 Oxygen ($^{18}O$) and Deuterium ($^{2}H$)

The isotopic composition of fluids combined with the major ions can provide information on the sub-surface processes occurring in geothermal systems. The δD and $\delta^{18}O$ values for thermal springs vary from −74.30 to −88.20‰ and −11.26 to −12.80‰, respectively. The δD and $\delta^{18}O$ values of cold and lake water samples vary from −64.38 to −79.24‰ and −8.21 to −11.77‰, respectively.

Most of the waters lie on, with a few exceptions plotted to the right of, the Global Meteoric Water Line of Craig (1961) and Kızılcahamam Meteoric Line of Pasvanoğlu and Çelik (2018), and therefore must be heated by deep circulation (Fig. 7). This indicates that the thermal waters have a meteoric origin, consistent with the conceptual model of thermal water discharge in the Çamlıdere area.

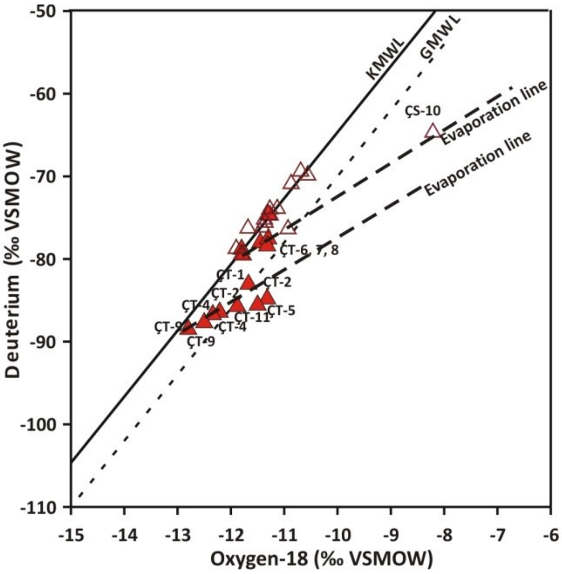


**Figure 7. Hydrogen and oxygen of Çamlıdere waters plotted to compare with the Kızılcahamam (KMWL; Pasvanoğlu and Çelik (2018)) and Global meteoric water line (GMWL)**

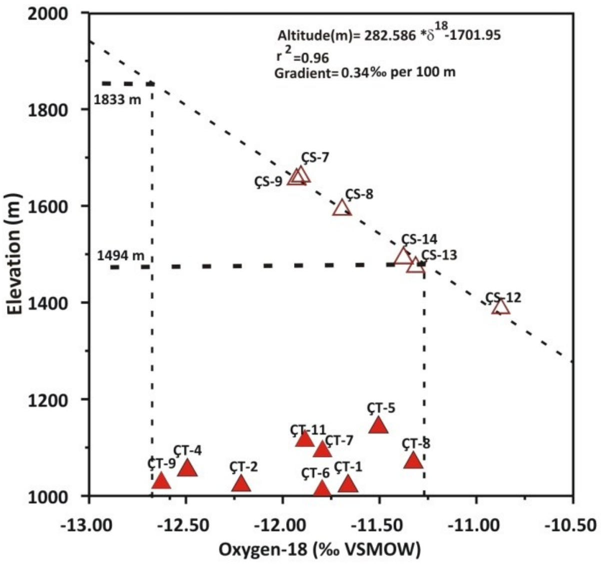


**Figure 8. Plot of $\delta^{18}O$ versus altitude of thermal waters in the Çamlıdere showing a decrease in $\delta^{18}O$ with increase in altitude**

Therefore, the average altitude of recharge can be derived from a negative, linear correlation between the elevation of the sample sites and their isotopic values. The regression equation computed from $\delta^{18}O$ with respect to elevation is:

$$h(m) = - h(m) = -282.586 * \delta^{18}O - 1701.95 \quad (r^2=0.96) \qquad (3)$$

Equation 3 show an apparent elevation effect on $\delta^{18}O$ on the order 0.34‰ per 100 m increase in elevation.

This allows estimating the recharge area of Çamlıdere thermal and/ or mineral waters from elevations between 1494-1833 m a.s.l. higher than that of the discharge area (Fig. 8). Groundwater flow in the volcanic rocks takes place through fractures and fissures. The general flow direction is from the high mountains to the basin of the Çamlıdere, i.e. from north to south (Fig 9).

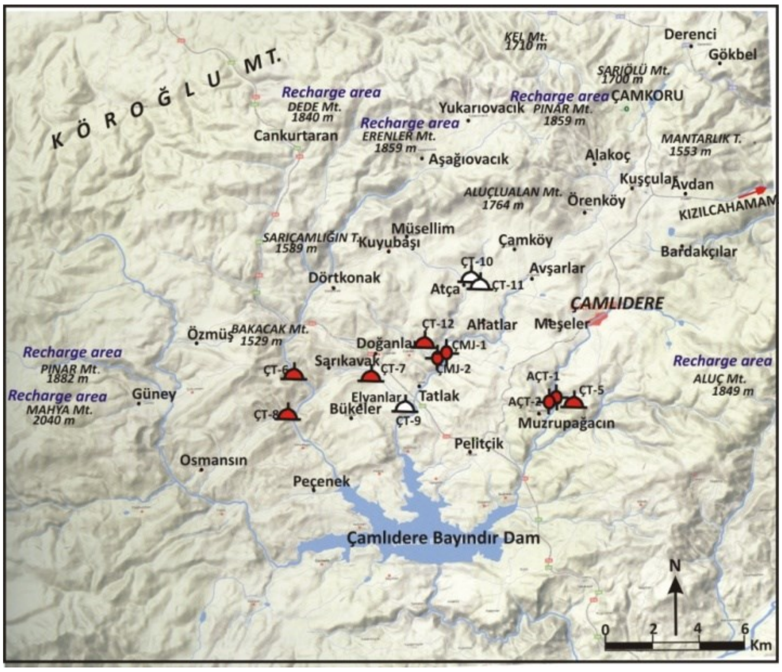


**Figure 9. Recharge areas of the Çamlıdere geothermal system.**

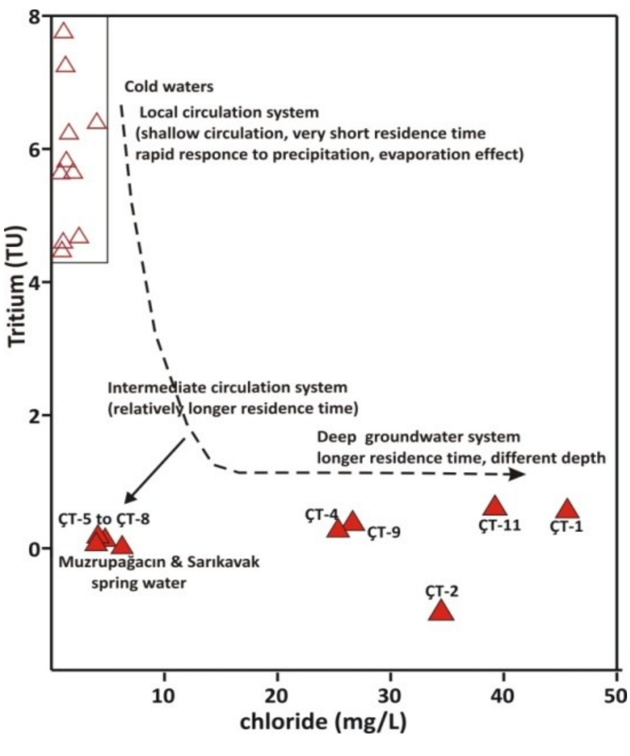


**Figure 10. A plot of Tritium versus $Cl^-$ (mg/L).**

4.4.2 Tritium

Groundwater circulation systems in the area are classified in their groups according to the chloride concentration and tritium content of cold and thermal waters (Fig. 10). Ahatlar and Muzrupağacın geothermal wells waters, Tatlak (ÇT-9) and Atca (ÇT-11) bicarbonate mineral waters, point to deep circulation paths, long residence time and/or more water-rock interaction process.

However, Muzrupağacın (ÇT-5) and Sarıkavak (ÇT-6 to ÇT-8) spring waters have low ionic concentrations, low temperature, low $^{3}H$ and low $Cl^-$, suggesting intermediate circulation system with relatively long residence time in an andesitic basaltic aquifer. These waters have been mixed with cold shallow-lying waters during their pathway to surface (Fig. 10).

This is also confirmed by water chemistry and temperatures of these waters. It is understood that the cold waters of Çamlıdere are represented by low chloride and EC values, enrichment in $\delta^{18}O$ and tritium high contents consistent with their relatively short residence times (Fig 10).

**5. CONCEPTUAL MODEL OF ÇAMLIDERE GEOTHERMAL SYSTEM**

The conceptual model of Çamlıdere geothermal system has been evaluated using hydrogeology, hydrochemistry, and environmental isotope studies together with regional geological structure (Fig. 11). Geothermal springs at Çamlıdere occur in an area of Miocene volcanics consisting of altered andesites, basalts and pyroclastic products.

The hydrothermal systems overlie a magma chamber, a source of heat and ascending magmatic fluids. Infiltrating meteoric waters also recharge these systems and are mineralised by water-rock-gas interactions as they flow through the volcanics.

Meteoric water which recharges the reservoir is heated with increasing geothermal gradient and moves up to the surface through the ES, E-W, NW trending faults and fractures which act as the hydrothermal conduit for thermal springs due to density difference, gas content and hydrodynamic effects of the fluids.

Due to their high permeability characterised by a network of joints, fractures, faults and karstic features of Paleozoic marbles and Mesozoic limestone below the Neogene units are likely reservoir rocks. Fault and fractures of lavas in the area have good aquifer characteristics, being a good target for thermal water drilling.

The Çamlıdere reservoir rocks have low permeability but are transected by a number of faults, damage zones, and fractures that provide leakage of thermal fluids to reach the surface. Such a 'system' is not associated with an impermeable cap, although fractured strata still exhibit low permeability as indicated by the output of the Ahatlar and Muzrupağacın geothermal wells.

The recharge rate in the area is quite large related to the permeability of the rocks. The elevation range supported by structural data suggests that the Çamlıdere thermal waters are recharged from the Aluç Mt. located in the east and the Mahya Mt. located in the west of Çamlıdere. The general flow is from the high mountains to the basin of the Çamlıdere, i.e. from N to S and from E to W.

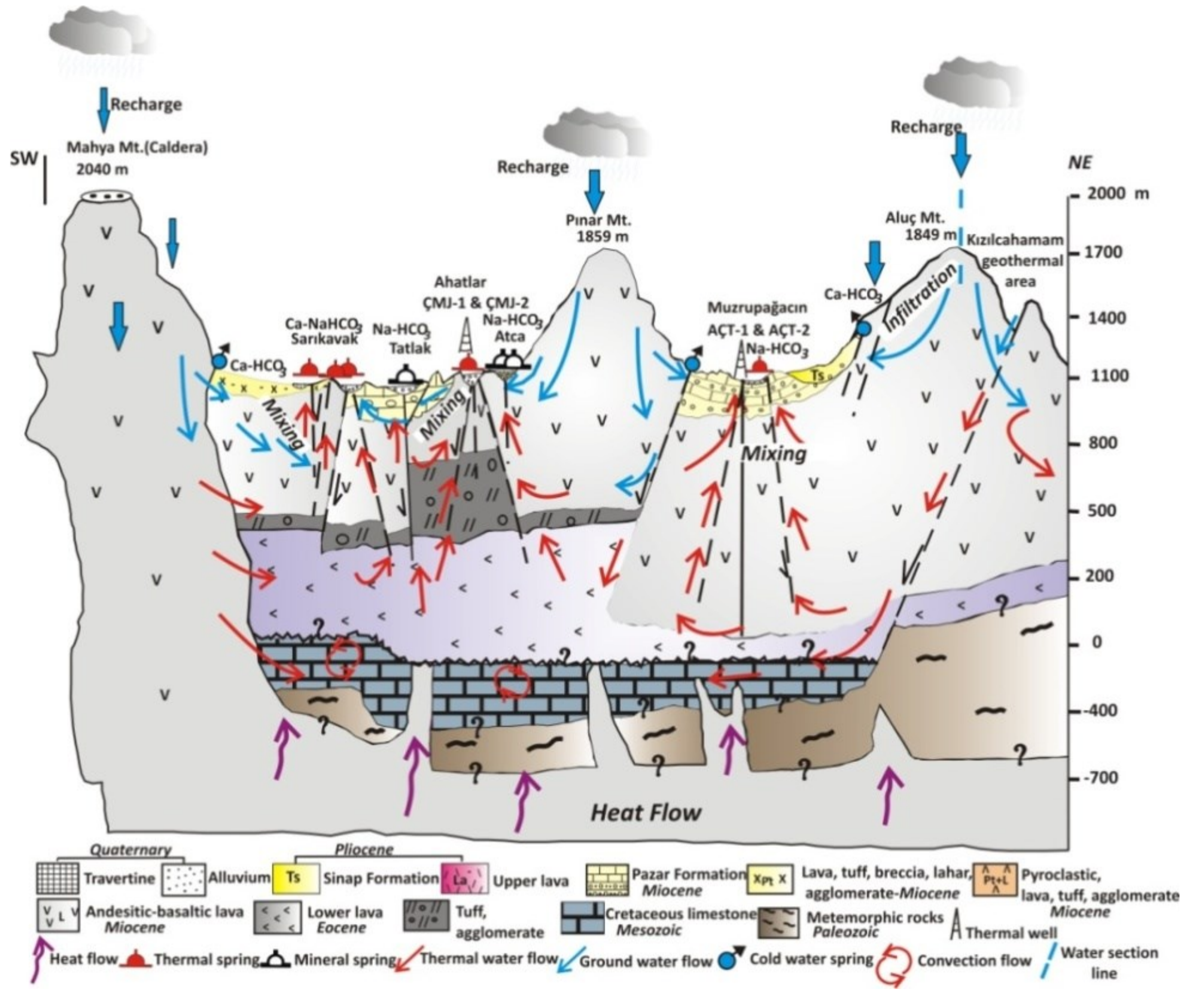


**Figure 11. A Conceptual model of groundwater flow systems in the Çamlıdere geothermal area.**

## 6. CONCLUSION

Thermal and mineral waters are of Na–$HCO_3$ type and Ca-Na-$HCO_3$ type waters, which confirms the influence of the geological formations dominated by Tertiary age volcanic and sedimentary rocks, attributable to the variability of the lithological composition and relating to different hydrogeological systems.

Chemical geothermometry (K-Mg, quartz) and lack of $\delta^{18}O$ enrichment indicate reservoir temperatures between 100 to–150 °C for the Çamlıdere area. The observed $SiO_2$ values and inferred T(K-Mg) data indicate some advective (terrain controlled) shallow flows involving $SiO_2$ re-equilibration of mixed thermal fluids.

By using a simple reservoir assessment, the total natural heat loss was found to be low (< 1MW th for all thermal springs and up to approximately 6 MW for all artesian wells). The estimates indicate a system with limited convective up-flow.

The Çamlıdere prospect hosts a low temperature, the fracture-zone system with limited convective up-flow and dominant conductive heat transfer from a resource base in the upper crust to the surface.

Isotopic data of Çamlıdere thermal waters ($\delta^{18}O$, $\delta^{2}H$, $\delta^{3}H$) reflect their deep-circulating meteoric origin and indicate recharge areas between 1494 and 1833 m a.s.l. Such levels are supported by structural data and suggest that Çamlıdere thermal waters are recharged from the Aluç Mt. in the east and the Mahya Mt. to the west of Çamlıdere.

Isotopic values indicate a common recharge area (elevation) for deep groundwaters, but with a different path, lengths flow to account for their variations in conductivity. The geochemical results and conceptual model of this study contribute to the development of resources at individual sites in each region.

Çamlıdere is located 27 km west of Kızılcahamam, and it's surrounded by forests, plateau and mountains, it is clear that thermal tourism in the area will be rapidly developed if the necessary investment is made.

Atca mineral water is very tasty. Its chemical composition is composed of Na, $HCO_3$ and $CO_2$. Once the necessary facilities are established, this mineral water should be bottled immediately. This attempt will promote evaluation of other mineral waters around the Çamlıdere area.

Development and widening of thermal water facilities in the Çamlıdere area are no doubt dependent on drilling of deep wells and thus increasing of hot water discharge. There is such potential in the study area and proposed project and investments should be started at once.

## ACKNOWLEDGEMENT

This study is financially supported in part by the Research Foundation of the Ankara University (Project No. 13L4343011). The authors thank the municipality Çamlıdere for their help and contribution throughout the study period.

## REFERENCES

Blattner, P.: Isotope Shift Data and The Natural Evolution of Geothermal Systems, *Chemical Geology*, **49**, (1985), 187–203.

Bülbül, E., Kuzuca, M., Arıgün, Z., Toprak, M., Toy, E., Kar, H., ve Mavi, I.: Ankara ve Civarı Jeotermal Enerji Aramaları Kapsamında, Ankara-Çamlıdere Tatlak, Muzrupağacın AÇT-2012/8 Sondajı ve Su Analizi Sonucu, MTA, Ankara Proje No.

(2002), 33-13-05-7, 3 s. [in Turkish]

Bülbül, E., Purtul, E., Toy, E., Yolal, A., ve Bal, E.: Ankara ve Civarı Jeotermal Enerji Aramaları Kapsamında, Ankara-Çamlıdere Muzrupağacın AÇT-2012/17 nolu Kuyu Bitirme Logu, MTA, Ankara ,Proje No. (2012), 1 s. [in Turkish]

Craig, H.: Isotopic variations in meteoric waters, *Science* **133**, (1961), 1702–1703.

Erişen, B.,and Ünlü, M.R.: Ankara, Çubuk, Kızılcahamam ve Kazan Alanının Jeolojisi ve Jeotermal Enerji Olanakları, MTA Report No. 9949, (1980) pp. 71 s Ankara [in Turkish].

Erol, O., 1954. Ankara ve Civarının Jeolojisi Hakkında Rapor, Kızılcahamam Güneyi Ankara Bala, Haymana Kırıkkale Çubuk, MTA, Derleme Raporu, No. 2491, s102-104, Ankara.

Fournier, R.O.: Silica in Thermal Waters. Laboratory and Field Investigations. Proceedings of The International Symposium on Hydrogeochemistry and Biochemistry. Tokyo, I. Clark Co., Washington DC (1973), pp. 122–139.

Giggenbach, W.F.: Geothermal Solute Equilibrium. Derivation of Na-K-Mg-Ca Geoindicators, *Geochimica et Cosmochimica Acta*, **52**, 2749-765, NITAR/UNDP Publication, Rome, (1988), 119–142.

Güleç, N.: Geochemistry of Geothermal Water and Its Relation to The Volcanism in The Kızılcahamam Ankara Area, (Turkey), *Journal of Volcanology and Geothermal Research*, **59**, (1994), 295–312.

Hochstein, M.P.: Geophysical Exploration of The Kamojang Geothermal Field, W. Java. Proceedings 2nd UN Symposium on Development of Geothermal Resources, (1975) 1049–1058.

ILBank.: Çamlıdere-Ahatlar (Ankara) Bölgesi Jeotermal Sular Kuyu Bitirme Raporu, Ankara (2009) [in Turkish].

Matsuhisa, Y., and Utada, M.: Oxygen Isotopic Study of Hydrothermally Altered Rocks From The Western Area of The Kuroko Mineralization in Hokuroku, NE Japan, *Proceedings*, IV International Water-Rock Interaction Symposium, Misasa, Japan, (1983) 317-320.

Pasvanoğlu, S. Çelik, M. Arıgün, and Güler, S.: A comparison of Hydrothermal Characteristics of Newly Discovered Çamlıdere Geothermal Field and The Kızılcahamam Geothermal Field, Central Anatolia, Turkey, World Geothermal Conference WGC2015 (2015).

Pasvanoğlu, S.: Hydrogeochemical and Isotopıc Investigation of Thermal and Mineralized Waters in the Vicinity of Kızılcahamam-Çamlıdere (Ankara). PhD Thesis. Ankara University, Ankara 315 p. [in Turkish, Unpublished].

Pasvanoğlu, S., Çelik, M.: A conceptual Model For Groundwater Flow and Geochemical Evolution of Thermal Fluids at The Kızılcahamam Geothermal Area, Galatian Volcanic Province, *Geothermics* **71**, (2018), 81–107.

Pasvanoğlu, S., Çelik, M.: Hydrogeochemical Characteristics and Conceptual Model of Çamlıdere Low Temperature Geothermal Prospect, Northern Central Anatolia, ISSN-0375-6505. *Geothermics* **79,** (2019), 82-104.

Tatlı, S.: Kızılcahamam Doğu Alanın Jeolojisi ve Jeotermal Enerji Olanakları, Mineral Research and Exploration Institute (MTA) of Turkey, Ankara, Report No. 5749, (1975) [in Turkish, Unpublished].

Toprak, V., Savaşcın, Y., Güleç, N., and Tankut, A.: Structure of the Galatian Volcanic Province Turkey, *International Geology Review* **38**, (1996), 747–758.

Türkecan, A., Hepşen, N., Papak, I., Akbaş, B., Dinçel, A., Karataş, S., Özgür, I., Akay, E.,Bedi, Y., Sevin, M., Mutlu, G., Sevin, D., Ünay, E., and Saraç, G.: Seben-Gerede (Bolu)-Güdül-Beypazarı (Ankara) ve Çerkeş-Orta-Kurşunlu (Çankırı) Yörelerinin (Köroğlu Dağları) Jeolojisi ve Volkanik Kayaçların Petrolojisi, Mineral Research and Exploration Institute (MTA) of Turkey, Ankara, Report No. 9193, (1991) [in Turkish, Unpublished].

Yurtsever, M., and Gat, J.R.: Atmospheric Waters, In: Stable Isotope Hydrology: Deuterium and Oxygen-18 in The Water Cycle. IAEA Technical Report Series, **210**, (1981), 103-142.

**Table 1. Results of chemical compositions of thermal and mineral waters from the study area**

| Nr | Date | T °C | pH | EC µS/cm | $Ca^{2+}$ | $Mg^{2+}$ | $Na^{+}$ | $K^{+}$ | $Cl^{-}$ | $SO_4^{2-}$ | $HCO_3^{-}$ | $SiO_2$ | F | B |
|---|---|---|---|---|---|---|---|---|---|---|---|---|---|---|
| *ÇT-1 | 5.11.2013 | 27 | 6.62 | 3240 | 75.98 | 8.86 | 770.60 | 91.24 | 45.73 | 8.49 | 2172 | 79.57 | 7.06 | 5.80 |
| | 8.4.2014 | | 6.60 | 3016 | 60.23 | 7.27 | 701.46 | 93.06 | 44.10 | 10.48 | 1960 | 88.10 | 7.31 | 6.38 |
| *ÇT-2 | 5.11.2013 | 42 | 6.31 | 1405 | 41.02 | 7.80 | 388.70 | 42.05 | 34.70 | 6.28 | 1293 | 140 | 3.70 | 4.90 |
| | 8.4.2014 | | 6.20 | 1669 | 43.03 | 10.32 | 325.32 | 50.36 | 23.71 | 7.35 | 1011 | 141.0 | 1.30 | 2.82 |
| *ÇT-3 | ▪4.10.2012 | 40 | 7.30 | 1245 | 47 | 8.87 | 310 | 41.80 | 17.5 | 9.10 | 996 | 117 | 0.70 | 1.40 |
| *ÇT-4 | 5.11.2013 | 37 | 6.96 | 2460 | 40 | 10.39 | 513.32 | 40.52 | 26.51 | 15.58 | 1603 | 76.14 | 0.76 | 3.28 |
| | 8.4.2014 | | 6.94 | 2090 | 41.79 | 6.51 | 527.01 | 37.46 | 28.25 | 8.51 | 1458 | 70 | 0.27 | 2.09 |
| ÇT-5 | 5.11.2013 | 25 | 6.90 | 335 | 19 | 9.10 | 55.00 | 17 | 4.70 | 3.50 | 240 | 100 | 0.20 | 0.20 |
| | 8.4.2014 | | 7.00 | 377 | 26.71 | 9.73 | 49.66 | 11.12 | 3.85 | 3.28 | 249.95 | 50 | 0.18 | <0.01 |
| ÇT-6 | 5.11.2013 | 28 | 7.80 | 410 | 29.10 | 8.55 | 37.41 | 21.84 | 4.16 | 5.55 | 233.54 | 74.81 | 0.12 | 0.76 |
| | 8.4.2014 | | 7.60 | 370 | 21.28 | 8.14 | 37.04 | 24.68 | 3.01 | 5.71 | 214.24 | 70 | 0.06 | 0.01 |
| ÇT-7 | 5.11.2013 | 25 | 7.57 | 390 | 30.83 | 10.33 | 32.17 | 10.97 | 6.21 | 5.33 | 210.30 | 73.71 | 0.58 | 0.67 |
| | 8.4.2014 | | 7.50 | 385 | 30.75 | 10.10 | 30.15 | 10.90 | 5.5 | 6.60 | 215.30 | 75.20 | 0.58 | 0.60 |
| ÇT-8 | 5.11.2013 | 22 | 6.60 | 350 | 29.70 | 12.43 | 30.49 | 14.10 | 4.01 | 7.60 | 227.57 | 92 | 0.31 | <2.5 |
| | 8.4.2014 | | 6.61 | 398 | 31.46 | 14.06 | 29.15 | 13.98 | 3.83 | 7.36 | 233.89 | 95.11 | 0.16 | <2.5 |
| ÇT-9 | 5.11.2013 | 23 | 6.70 | 2250 | 86.90 | 25.52 | 408.69 | 83.30 | 25.42 | 19.95 | 1385.57 | 99.39 | 0.53 | 4.00 |
| | 8.4.2014 | | 6.70 | 1816 | 83.50 | 28.25 | 400.0 | 78.20 | 25.50 | 18.00 | 1390 | 100 | 0.50 | 4.10 |
| ÇT-10 | 5.11.2013 | 13 | 7.62 | 1390 | 55 | 7.00 | 470.10 | 52.00 | 26.10 | 7.20 | 1390 | 39.10 | 4.80 | 4.10 |
| | 8.4.2014 | | 6.20 | 2200 | 50.01 | 7.74 | 471.52 | 53.24 | 26.28 | 7.45 | 1393 | 38.48 | 4.79 | 3.58 |
| ÇT-11 | 5.11.2013 | 11 | 7.80 | 3550 | 119.49 | 16.67 | 703.48 | 75.06 | 39.09 | 10.36 | 2155 | 88.19 | 6.17 | 6.92 |
| | 8.4.2014 | | 7.50 | 3520 | 110 | 16.20 | 700 | 74.05 | 40.10 | 10.40 | 2160 | 80.20 | 6.10 | 6.91 |
| ÇT-12 | 5.11.2013 | 23 | 6.50 | 1650 | 42.00 | 8.90 | 330 | 50.0 | 22.00 | 8.00 | 1000 | 120 | 1.14 | 3.00 |
| | 8.4.2014 | | 6.23 | 1658 | 39.37 | 9.76 | 326.36 | 47.87 | 21.99 | 7.32 | 998.79 | 137.77 | 1.14 | 2.92 |

Concentrations are expressed in mg/L; *geothermal well; EC= Electric conductivity; ▪Results of M.T.A. Sample numbers correspond to localities shown in Fig. 1.

Most samples of springs and thermal wells in the table are 'mineral bicarbonate waters' since their $HCO_3$ content is > 600 mg/L.

**Table 2. Measured temperature, pH, coordinates of sample locations. Also shown are chemical compositions of cold waters from the study area**

| Nr | Date | T°C | pH | EC µS/cm | X | Y | Z | $Ca^{2+}$ | $Mg^{2+}$ | $Na^{+}$ | $K^{+}$ | $Cl^{-}$ | $SO_4^{2-}$ | $HCO_3^{-}$ | $SiO_2$ | F | B |
|---|---|---|---|---|---|---|---|---|---|---|---|---|---|---|---|---|---|
| ÇS-1 | 5.11.2013 | 11 | 8,63 | 73.3 | 4478685 | 0463611 | 1664 | 9.77 | 1.00 | 4.87 | 0.64 | 1.08 | 5.11 | 40.67 | 36.03 | 0.05 | 0.48 |
| ÇS-2 | 5.11.2013 | 16 | 6.68 | 374 | 4481410 | 046251 | 1453 | 26.96 | 8.83 | 49.60 | 11.67 | 4.01 | 3.98 | 261.85 | 26.08 | 0.20 | 0.01 |
| ÇS-3 | 5.11.2013 | 15 | 9.8 | 125 | 4479341 | 0461106 | 1696 | 10.86 | 1.70 | 4.09 | 2.43 | 1.91 | 7.32 | 46.48 | 51.39 | 0.05 | 1.02 |
| ÇS-4 | 8.4.2014 | 12 | 6.30 | 86 | 4481650 | 0450301 | 1054 | 9.43 | 1.73 | 3.25 | 3.18 | 1.55 | 9.43 | 35.71 | 25.08 | 0.10 | <0.01 |
| ÇS-5 | 8.4.2014 | 13 | 7.19 | 982 | 4479181 | 0442273 | 1048 | 143.39 | 72.87 | 6.78 | 7.91 | 2.44 | 174.02 | 574.29 | 25.54 | 0.14 | <0.01 |
| ÇS-6 | 5.11.2013 | 14 | 8.61 | 109 | 4479625 | 0438211 | 1400 | 12.87 | 3.28 | 3.91 | 2.04 | 1.32 | 4.36 | 58.10 | 42.92 | 0.03 | 0.55 |
| ÇS-7 | 5.11.2013 | 8 | 9.62 | 93.5 | 4484576 | 0449359 | 1112 | 12.66 | 1.07 | 3.98 | 1.45 | 1.25 | 4.20 | 46.77 | 31.36 | 0.04 | <0.25 |
| ÇS-8 | 8.4.2014 | 5 | 8.90 | 111.3 | 4488300 | 452200 | 1593 | 19.38 | 1.72 | 5.16 | 1.38 | 0.80 | 5.14 | 69.54 | 38.46 | 0.11 | <2.50 |
| ÇS-9 | 8.4.2014 | 6 | 8.04 | 71 | 4491937 | 454455 | 1669 | ● | ● | ● | ● | ● | ● | ● | ● | ● | ● |
| *ÇS-10 | 8.4.2014 | 13 | 7.3 | 280 | 4488246 | 442244 | 1122 | Lake | ● | ● | ● | ● | ● | ● | ● | ● | ● |
| ÇS-11 | 8.4.2014 | 16 | 7.3 | 509 | 4489129 | 459763 | 1446 | ● | ● | ● | ● | ● | ● | ● | ● | ● | ● |
| ÇS-12 | 8.4.2014 | 9 | 7.60 | 50.40 | 4489716 | 458257 | 1395 | ● | ● | ● | ● | ● | ● | ● | ● | ● | ● |
| ÇS-13 | 8.4.2014 | 8 | 7.87 | 139.70 | 4490490 | 447756 | 1481 | 20.03 | 4.14 | 4.19 | 1.42 | 1.04 | 2.21 | 88.50 | 37.94 | 0.16 | <2.5 |
| ÇS-14 | 8.4.2014 | 9 | 7.68 | 267 | 4492050 | 448962 | 1501 | 27.22 | 10.97 | 12.49 | 4.05 | 0.93 | 10.32 | 158.04 | 55.11 | 0.17 | <2.5 |

Sample numbers correspond to locality shown in Fig. 1; EC= Electric conductivity; Cation and anion concentration are in mg/L *ÇS-10: lake water; •indicate not measured; *Lake water.

ÇS-5 spring water classified as mineral bicarbonate waters' since $HCO_3$ content is > 600 mg/L.